Subspace-search variational quantum eigensolver for excited states

Ken M. Nakanishi [1,*] Kosuke Mitarai,[2,3,†] and Keisuke Fujii[2,4,‡]

[1]*Graduate School of Science, The University of Tokyo, 7-3-1 Hongo, Bunkyo-ku, Tokyo 113-0033, Japan*
[2]*Graduate School of Engineering Science, Osaka University, 1-3 Machikaneyama, Toyonaka, Osaka 560-8531, Japan*
[3]*QunaSys Incorporated, High-Tech Hongo Building 1F, 5-25-18 Hongo, Bunkyo, Tokyo 113-0033, Japan*
[4]*JST, PRESTO, 4-1-8 Honcho, Kawaguchi, Saitama 332-0012, Japan*

The variational quantum eigensolver (VQE), a variational algorithm to obtain an approximated ground state of a given Hamiltonian, is an appealing application of near-term quantum computers. To extend the framework to excited states, we here propose an algorithm, the subspace-search variational quantum eigensolver (SSVQE). This algorithm searches a low-energy subspace by supplying orthogonal input states to the variational ansatz and relies on the unitarity of transformations to ensure the orthogonality of the output states. The kth excited state is obtained as the highest-energy state in the low-energy subspace. The proposed algorithm consists only of two parameter optimization procedures and does not employ any ancilla qubits. The avoidance of the estimation of the inner product and the small number of procedures required are considerable improvements from the existing proposals for excited states, making our proposal an improved near-term quantum algorithm. We further generalize the SSVQE to obtain all excited states up to the kth by only a single optimization procedure. From numerical simulations, we verify the proposed algorithms. This work extends the applicable domain of the VQE to excited states and their related properties as a transition amplitude without sacrificing any of its feasibility. Moreover, the proposed variational subspace search, which generalizes the state search problem to the search of a unitary mapping to a specific subspace, itself would be useful for various quantum information processing methods such as finding a protected subspace or a good variational quantum error correction code.

I. INTRODUCTION

Supported by the worldwide active research for the development of quantum devices, quantum computers equipped with almost a hundred qubits are now within reach. Those near-term quantum computers are often called noisy intermediate-scale quantum (NISQ) devices [1], reflecting the fact that those quantum computers are not fault tolerant, that is, they do not have a guaranteed accuracy of the computational result. However, such a NISQ device is believed not to be simulatable on classical computers if the gate fidelity is sufficiently high [2–4]. This fact encourages us to look for practical applications of them.

The variational quantum eigensolver (VQE) [5–7] is an attracting application of near-term quantum computers in the hope that the controllable quantum devices can simulate another quantum system more efficiently than classical devices. The VQE is an algorithm for finding an approximate ground state of a given Hamiltonian $\mathcal{H}$. For this purpose, the VQE

utilizes a parametrized quantum circuit $U(\boldsymbol{\theta})$, which is also called an ansatz circuit, to generate an ansatz state $|\psi(\boldsymbol{\theta})\rangle$. The expectation value of the target Hamiltonian $\langle\mathcal{H}(\boldsymbol{\theta})\rangle = \langle\psi(\boldsymbol{\theta})|\mathcal{H}|\psi(\boldsymbol{\theta})\rangle$ is minimized by iterative optimization of the parameters $\boldsymbol{\theta}$. The circuit with the resultant optimal parameters $\boldsymbol{\theta}^*$ which minimizes $\langle\mathcal{H}\rangle$ outputs the approximate ground state.

Not only is the ground state, which the original VQE aims to find, but also excited states of molecules are responsible for many chemical reactions and physical processes. For example, the transition between a ground state and excited states is the origin of luminescence [8]. Intermediate states of a chemical reaction are, in general, not a ground state of a system, and therefore the properties of such excited states are important for an analysis of them [9].

In spite of the importance of the excited states, classical computation suffers from increasing computational cost and gives relatively poor results for them [9–11]. This motivates us to utilize quantum computers for the task of finding excited states and analyzing their property. A long-term quantum algorithm for a chemical reaction has been investigated in Ref. [12]. However, algorithms which we can run on NISQ devices are yet to appear.

In order to find the excited states using NISQ devices, we propose a method which utilizes the conservation of orthogonality under the unitary transformation. We call the method the subspace-search VQE (SSVQE). The SSVQE takes two or more orthogonal states as inputs to a parametrized quantum

*ken-nakanishi@g.ecc.u-tokyo.ac.jp
†mitarai@qc.ee.es.osaka-u.ac.jp
‡fujii@qc.ee.es.osaka-u.ac.jp

circuit, and minimizes the expectation value of the energy in the space spanned by those states. This method automatically imposes the orthogonality condition on the output states, and therefore allows us to remove the requirement to estimate the inner product of the quantum states, which has been employed in the previous works [13,14] to ensure orthogonality. In principle, the proposed algorithm can find the kth excited state by running optimization of the circuit parameters only twice. We also propose a generalized version of the SSVQE, which finds all excited states up to the kth by running only one optimization procedure. As a possible application of the SSVQE, a method to measure a transition amplitude between two eigenstates is also described. It can evaluate material properties such as the permittivity and rate of spontaneous emission. We perform numerical simulations and show the validity of the proposed algorithms for fully connected random transverse Ising models and helium hydride. This work greatly extends the practicability of the VQE by enabling it to find the excited states efficiently, and thereby further promotes the VQE as a candidate for a possible application of NISQ devices.

The rest of the paper is organized as follows. In Sec. II we first propose the algorithm of the SSVQE and its extended version. Then, in Sec. III we briefly review the existing works addressing the same objective of finding the excited states in the framework of the VQE. An algorithm to obtain the transition amplitude is described in Sec. IV. Finally, we present the simple, proof-of-principle numerical simulations in Sec. V.

II. METHODS

The VQE is a quantum-classical hybrid algorithm to find a ground state of a given Hamiltonian $\mathcal{H}$ using NISQ devices. For this purpose, the VQE utilizes a parametrized quantum circuit $U(\boldsymbol{\theta})$, also called an ansatz circuit, to generate an ansatz state $|\psi(\boldsymbol{\theta})\rangle$. The expectation value of the target Hamiltonian $\langle\mathcal{H}(\boldsymbol{\theta})\rangle = \langle\psi(\boldsymbol{\theta})|\mathcal{H}|\psi(\boldsymbol{\theta})\rangle$ is minimized by an iterative optimization of the parameters $\boldsymbol{\theta}$.

We generalized the state-searching problem to the subspace-searching one by variationally finding a unitary transformation that maps a subspace into another. This general protocol would be useful for quantum information processing on the near-term quantum devices beyond the excited states. Our objective here is to find excited states of the Hamiltonian $\mathcal{H}$. Since the eigenstates of the Hamiltonian $\mathcal{H}$ are mutually orthogonal, a straightforward construction of the algorithm to find the kth excited state is to minimize $\langle\mathcal{H}(\boldsymbol{\theta})\rangle$ by imposing an orthogonality condition between the ansatz state $|\psi(\boldsymbol{\theta})\rangle$ and all of the ground/excited states up to the $(k-1)$th. By inductively repeating this, we can find the excited states of interest. This strategy which measures the inner product between the ansatz state and all of the ground/excited states up to $(k-1)$th has been employed to ensure the orthogonality in previous works [13,14]. Nonorthogonal components cannot be removed beyond the accuracy determined by the number of measurements. In contrast, the SSVQE and the weighted SSVQE we propose here utilize the conservation of orthogonality under the unitary transformation in an effort to satisfy the orthogonality condition. These methods automatically

impose the orthogonality on the output states, and therefore remove the requirement to estimate the inner products.

A. Subspace-search variational quantum eigensolver

The key idea is to ensure the orthogonality at the *input* of the quantum circuit, not at the output. Below, we describe the algorithm to find the kth excited state that works on an n-qubit quantum computer. We define the ground state as the 0th excited state. The algorithm, which we refer to as the subspace-search VQE (SSVQE), runs as follows.

Algorithm:

(1) Construct an ansatz circuit $U(\boldsymbol{\theta})$ and choose input states $\{|\varphi_j\rangle\}_{j=0}^{k}$ which are mutually orthogonal ($\langle\varphi_i|\varphi_j\rangle = \delta_{ij}$).

(2) Minimize $\mathcal{L}_1(\boldsymbol{\theta}) = \sum_{j=0}^{k}\langle\varphi_j|U^\dagger(\boldsymbol{\theta})\mathcal{H}U(\boldsymbol{\theta})|\varphi_j\rangle$. We denote the optimal $\boldsymbol{\theta}$ by $\boldsymbol{\theta}^*$.

(3) Construct another parametrized quantum circuit $V(\boldsymbol{\phi})$ that only acts on the space spanned by $\{|\varphi_j\rangle\}_{j=0}^{k}$.

(4) Choose an arbitrary index $s \in \{0, \ldots, k\}$, and maximize $\mathcal{L}_2(\boldsymbol{\phi}) = \langle\varphi_s|V^\dagger(\boldsymbol{\phi})U^\dagger(\boldsymbol{\theta}^*)\mathcal{H}U(\boldsymbol{\theta}^*)V(\boldsymbol{\phi})|\varphi_s\rangle$.

We note that, in practice, the input states $\{|\varphi_j\rangle\}_{j=0}^{k}$ can be chosen from a set of states which are easily preparable, such as the computational basis.

Let the set of eigenstates of $\mathcal{H}$ be $\{|E_j\rangle\}_{j=0}^{2^n-1}$ with corresponding eigenenergies $\{E_j\}_{j=0}^{2^n-1}$ where $E_i \geqslant E_j$ when $i \geqslant j$. Then, the circuit optimized at step (2) of the above algorithm is a unitary that best approximates the mapping from the space spanned by $\{|\varphi_j\rangle\}_{j=0}^{k}$ to the one spanned by $\{|E_j\rangle\}_{j=0}^{k}$. Therefore, in step (2), we can find the subspace which includes $|E_k\rangle$ as the highest-energy state, using a carefully constructed ansatz $U(\boldsymbol{\theta})$. The unitary $V(\boldsymbol{\phi})$ is responsible for searching in that subspace. By maximizing $\mathcal{L}_2(\boldsymbol{\phi})$, we find the kth excited state $|E_k\rangle$.

In the case of $k \geqslant 2^{n-1}$, it is faster to choose $2^n - k$ of the orthogonal input states $|\varphi_j\rangle$ and maximize $\mathcal{L}_1(\boldsymbol{\theta})$ instead of minimizing it in step (2), then minimize $\mathcal{L}_2(\boldsymbol{\theta})$ instead of maximizing it in the final step.

B. Weighted SSVQE for finding the kth excited state

Here, we extend the algorithm described in the previous section to find the kth excited state of a given Hamiltonian which requires only a single optimization procedure. It runs as follows.

Algorithm:

(1) Construct an ansatz circuit $U(\boldsymbol{\theta})$ and choose input states $\{|\varphi_j\rangle\}_{j=0}^{k}$ which are orthogonal with each other ($\langle\varphi_i|\varphi_j\rangle = \delta_{ij}$).

(2) Minimize $\mathcal{L}_w(\boldsymbol{\theta}) = w\langle\varphi_k|U^\dagger(\boldsymbol{\theta})\mathcal{H}U(\boldsymbol{\theta})|\varphi_k\rangle + \sum_{j=0}^{k-1}\langle\varphi_j|U^\dagger(\boldsymbol{\theta})\mathcal{H}U(\boldsymbol{\theta})|\varphi_j\rangle$, where the weight w can be any value in $(0, 1)$.

When the cost $\mathcal{L}_w$ reaches its global optimum, the circuit $U(\boldsymbol{\theta})$ becomes a unitary which maps $|\varphi_k\rangle$ to the kth excited state $|E_k\rangle$ of the Hamiltonian and others to the subspace spanned by $\{|E_j\rangle\}_{j=0}^{j=k-1}$. Therefore, by minimizing the cost $\mathcal{L}_w$, we can find the kth excited state by a single optimization process. Note that the overall time required for the optimization might increase, due to the more complicated landscape of the cost function.

C. Weighted SSVQE for finding up to the kth excited states

We further generalize the above argument and propose an algorithm for finding all excited states of a given Hamiltonian up to the kth with only one optimization procedure.

Algorithm:

(1) Construct an ansatz circuit $U(\boldsymbol{\theta})$ and choose input states $\{|\varphi_j\rangle\}_{j=0}^{k}$ which are orthogonal with each other ($\langle\varphi_i|\varphi_j\rangle = \delta_{ij}$).

(2) Minimize $\mathcal{L}_{\boldsymbol{w}}(\boldsymbol{\theta}) = \sum_{j=0}^{k} w_j \langle\varphi_j|U^\dagger(\boldsymbol{\theta})\mathcal{H}U(\boldsymbol{\theta})|\varphi_j\rangle$, where the weight vector $\boldsymbol{w}$ is chosen such that $w_i > w_j$ when $i < j$.

The weight vector introduced here has the effect of choosing which $|\varphi_j\rangle$ is converted to which excited state. It is easy to see the circuit $U(\boldsymbol{\theta})$ when the cost $\mathcal{L}_{\boldsymbol{w}}$ reaches its global optimum becomes a unitary which maps $|\varphi_j\rangle$ to the jth excited state $|E_j\rangle$ of the Hamiltonian for each $j \in \{0, 1, \ldots, k\}$. We provide a proof in the Appendix. In this case, too, note that the overall time required for the optimization might increase due to the same reason as the previous section.

III. RELATED WORKS

In this section, we first overview previous works, and then describe the advantages of our methods.

Reference [15] has proposed a method which hybridizes the quantum phase estimation algorithm and the VQE. Although it is experimentally demonstrated [15], the method is unlikely to be implemented on a NISQ device, due to the need for the controlled time evolution.

In Ref. [16], a method called quantum subspace expansion has been proposed. The algorithm first finds the ground state $|E_0\rangle$ by the usual VQE protocol, and then measures the matrix elements of the Hamiltonian with respect to the space spanned by $\{O_\alpha|E_0\rangle\}$, where $\{O_\alpha\}$ is a set of excitation operators. The diagonalization of the matrix, which is done classically, can determine the approximate eigenvalue spectra. They have used a set of one electron excitation operators $\{a_v^\dagger a_o\}$, where $a_i^\dagger$ and a_j are the fermion creation and annihilation operators, respectively, and i, j running all possible indices, for $\{O_\alpha\}$.

The constrained VQE proposed in Ref. [17] can also be used for finding a certain set of excited states. They proposed a way to introduce constraints, such as the number of electrons or the overall spin of the system, on the VQE. The introduction of the constraints is done by adding the penalty term to the cost function. Their method finds the lowest-energy state under the constraints. Since the difference in the constraints, such as the difference in the number of electrons or the overall spins, generally changes the energy of the system, it can be utilized to find a certain set of excited states.

Reference [13] has recently proposed an inductive method which adds a penalty term to ensure the orthogonality of the ansatz state with respect to the low-lying state. To be more concrete, to find the kth excited state, they use $\langle\mathcal{H}(\boldsymbol{\theta}_k)\rangle + \sum_{i=0}^{k-1} \beta_i|\langle\psi(\boldsymbol{\theta}_k)|\psi(\boldsymbol{\theta}_i^*)\rangle|^2$, where $\boldsymbol{\theta}_i^*$ is the optimal parameters for the ith excited state and β_i is a hyperparameter that determines the strength of the penalty, as the target cost function to be minimized by tuning $\boldsymbol{\theta}_k$. Their method estimates the inner products of the quantum states. As stated earlier, nonorthogonal components cannot be removed beyond the
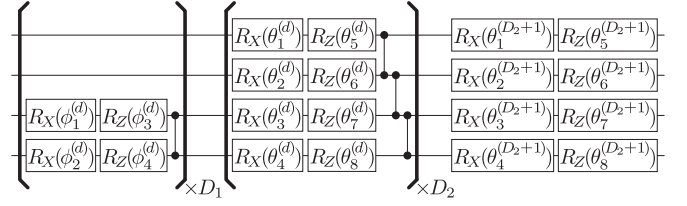

FIG. 1. Variational quantum circuit used in the simulations of Sec. V. These parameters $\boldsymbol{\phi}, \boldsymbol{\theta}$ are optimized to to minimize $\mathcal{L}$. D_1 and D_2 denote the number of repetitions of a circuit in each bracket. Note that, in the explanation of weighted SSVQE, $\boldsymbol{\theta}$ denotes $\{\boldsymbol{\phi}, \boldsymbol{\theta}\}$ in this figure.

accuracy determined by the number of measurements. Their method works well when the hyperparameter β_i is set properly as shown in Ref. [13]. Reference [14] has enabled the optimization by the imaginary time evolution of the parameters in this approach.

The advantages of our methods, when compared to the methods above, are as follows.

(1) The energy spectrum found by the SSVQE or the weighted SSVQE is exact when $U(\boldsymbol{\theta})$ and $V(\boldsymbol{\phi})$ have the ability to represent the exact unitary which maps the k input states to the k eigenstates of the Hamiltonian.

(2) The estimation of the inner product of quantum states is not employed and thus easily implementable on the NISQ devices.

(3) In the SSVQE, there are no hyperparameters.

(4) In the weighted SSVQE, the results are unique regardless of the value of the hyperparameters if they meet the conditions.

(5) Optimization runs only twice for the SSVQE and only once for the weighted SSVQE.

IV. CALCULATION OF TRANSITION MATRIX ELEMENTS

It is possible to measure a transition amplitude of an operator A, $\langle E_i|A|E_j\rangle$, using the result of the SSVQE. Note that $\langle E_i|A|E_j\rangle = \langle\varphi_i|U^\dagger(\boldsymbol{\theta}^*)AU(\boldsymbol{\theta}^*)|\varphi_j\rangle$, where $U(\boldsymbol{\theta}^*)$ is the optimized unitary. We can measure this by expanding it as

$$
\begin{aligned}
&\mathrm{Re}(\langle\varphi_i|U^\dagger(\boldsymbol{\theta}^*)AU(\boldsymbol{\theta}^*)|\varphi_j\rangle) \\
&= \langle+_{ij}^x|U^\dagger(\boldsymbol{\theta}^*)AU(\boldsymbol{\theta}^*)|+_{ij}^x\rangle \\
&\quad - \tfrac{1}{2}\langle\varphi_i|U^\dagger(\boldsymbol{\theta}^*)AU(\boldsymbol{\theta}^*)|\varphi_i\rangle \tfrac{1}{2}\langle\varphi_j|U^\dagger(\boldsymbol{\theta}^*)AU(\boldsymbol{\theta}^*)|\varphi_j\rangle,
\end{aligned}
\tag{1}
$$

$$
\begin{aligned}
&\mathrm{Im}(\langle\varphi_i|U^\dagger(\boldsymbol{\theta}^*)AU(\boldsymbol{\theta}^*)|\varphi_j\rangle) \\
&= \langle+_{ij}^y|U^\dagger(\boldsymbol{\theta}^*)AU(\boldsymbol{\theta}^*)|+_{ij}^y\rangle \\
&\quad - \tfrac{1}{2}\langle\varphi_i|U^\dagger(\boldsymbol{\theta}^*)AU(\boldsymbol{\theta}^*)|\varphi_i\rangle - \tfrac{1}{2}\langle\varphi_j|U^\dagger(\boldsymbol{\theta}^*)AU(\boldsymbol{\theta}^*)|\varphi_j\rangle,
\end{aligned}
\tag{2}
$$

where $|+_{ij}^x\rangle = (|\varphi_i\rangle + |\varphi_j\rangle)/\sqrt{2}$ and $|+_{ij}^y\rangle = (|\varphi_i\rangle + i|\varphi_j\rangle)/\sqrt{2}$. Recall that in practice the input states are chosen from simple states such as the computational basis, and therefore we assume that the superpositions such as $|+_{ij}^x\rangle$ can easily be prepared. Each term of the above equation is measured
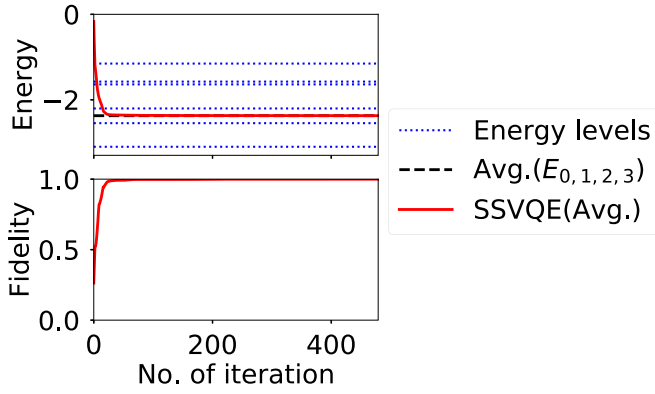
FIG. 2. Step (1) of the SSVQE to find the third excited state of a transverse Ising model. Black dashed line: Avg.$(E_{0,1,2,3}) = \frac{1}{4} \sum_{k=0}^{3} E_k$, which is the globally optimal value of $\mathcal{L}_1/4$ in this case. Red solid lines: The evolution of $\mathcal{L}_1/4$ and the fidelity (see the main text for the definition) during the optimization process.

separately on the NISQ device and then is summed up on a classical computer.

V. NUMERICAL SIMULATION

Here, we numerically simulate our algorithms with 4-qubit Hamiltonians. Figure 1 shows the variational ansatz used in the simulations. We chose the input states as $\{|\varphi_j\rangle\} = \{|0000\rangle, |0001\rangle, |0010\rangle, |0011\rangle\}$. The depth D_1 is set to $D_1 = 2$ for all of them. D_2 is set to $D_2 = 6$ for the SSVQE and the weighted SSVQE for finding the kth excited states, and $D_2 = 8$ for the weighted SSVQE for finding all excited states up to the kth. The initial values of the parameters were randomly sampled from a uniform distribution $[0, 2\pi)$. For each simulation, the optimization was run for ten times starting from different initial values. The results shown in the following sections are the ones which achieved the lowest value of the cost function among those ten results. We used the Broyden-Fletcher-Goldfarb-Shanno (BFGS) method [18] implemented in the SciPy library [19] for the optimization of the parameters.
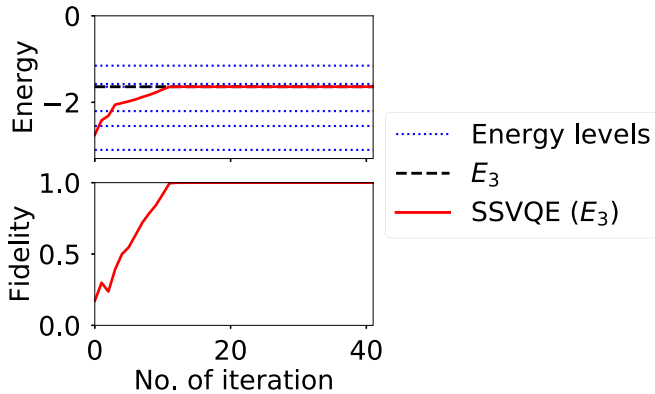

FIG. 3. Step (2) of the SSVQE to find the third excited state of a transverse Ising model. Red solid lines: The evolution of $\mathcal{L}_2$ and the fidelity (see the main text for the definition) during the optimization process.
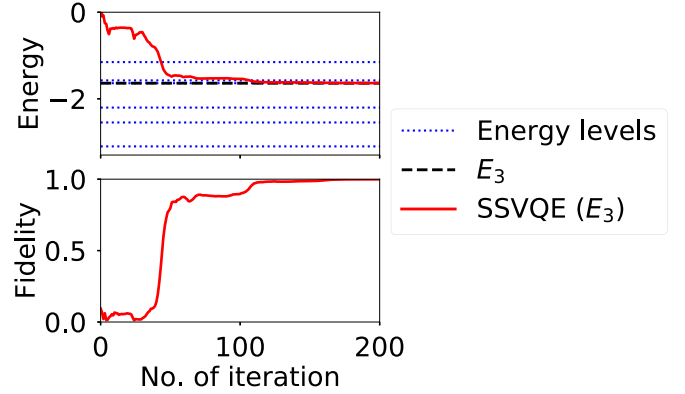

FIG. 4. The weighted SSVQE to find the third excited state of a transverse Ising model. In the energy diagram, SSVQE(E_3) (red solid line) is $\langle \varphi_3 | U^\dagger(\boldsymbol{\theta}) \mathcal{H} U(\boldsymbol{\theta}) | \varphi_3 \rangle$ at each iteration.

A. Transverse Ising model

First, we demonstrate our idea with a Hamiltonian of the fully connected transverse Ising model,

$$\mathcal{H} = \sum_{i=1}^{N} a_i X_i + \sum_{i=1}^{N} \sum_{j=1}^{i-1} J_{ij} Z_i Z_j, \tag{3}$$

with $N = 4$. The coefficients a_i and J_{ij} are sampled randomly from a uniform distribution on $[0, 1)$. In this section, we use one Hamiltonian with the same coefficients as an example. All experiments were conducted on the case of $k = 3$.

1. SSVQE

The SSVQE can find the kth excited state with only two optimization procedures. Figure 2 shows the first optimization process of $\boldsymbol{\theta}$ to minimize $\mathcal{L}_1(\boldsymbol{\theta})$. In Fig. 2, the fidelity is defined by the overlap between the space spanned by $\{|E_j\rangle\}_{j=0}^3$ and the output of the quantum circuit $\{U(\boldsymbol{\theta})|\varphi_j\rangle\}_{j=0}^3$, namely, $\frac{1}{4} \sum_{i=0}^{3} \sum_{j=0}^{3} |\langle E_i | U(\boldsymbol{\theta}) | \varphi_j \rangle|^2$. We see that, as the cost function gets close to its global minimum, the fidelity approaches unity as expected.

Figure 3 shows the second process of optimizing $\boldsymbol{\phi}$ to minimize $\mathcal{L}_2(\boldsymbol{\phi})$. Here, the fidelity is defined by
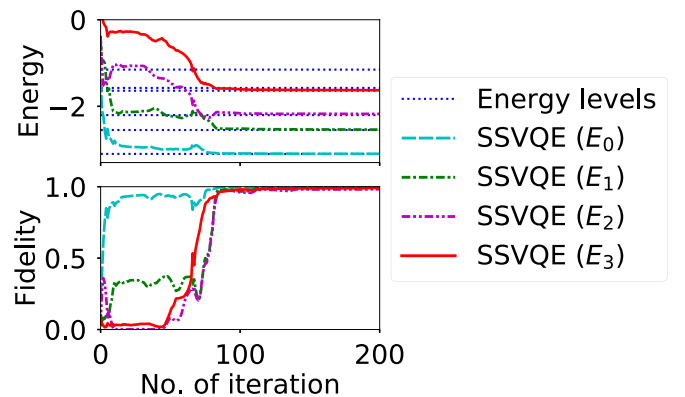

FIG. 5. The weighted SSVQE to find excited states of a transverse Ising model up to the third. In the energy diagram, SSVQE(E_k) ($k = 0, 1, 2, 3$) are $\langle \varphi_k | U^\dagger(\boldsymbol{\theta}) \mathcal{H} U(\boldsymbol{\theta}) | \varphi_k \rangle$ for each k at each iteration.
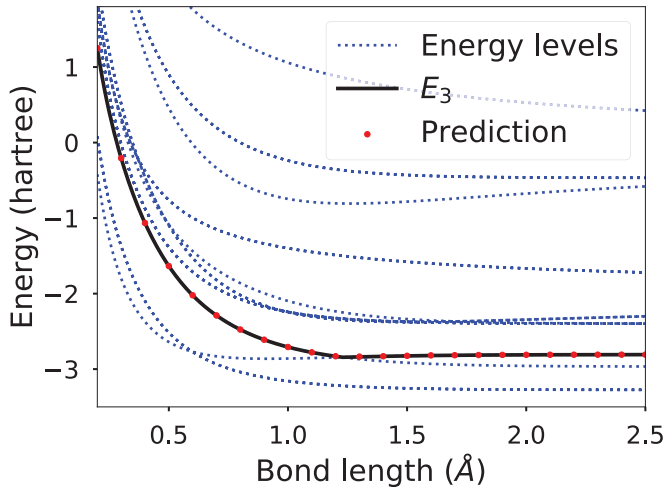
FIG. 6. The energy levels of the Hamiltonian of HeH and the calculated energy of the third excited state using the SSVQE.

$|\langle E_3|U(\boldsymbol{\theta}^*)V(\boldsymbol{\phi})|\varphi_3\rangle|^2$. One can see the subspace-search approach works well from Fig. 3.

2. Weighted SSVQE for finding the kth excited state

The method described in Sec. II B can find the kth excited state by only one optimization sequence. Here, we chose $w = 0.5$ as the weight. Figure 4 shows the optimization process of $\boldsymbol{\theta}$ to minimize $\mathcal{L}_w(\boldsymbol{\theta})$. Here, the fidelity is defined by $|\langle E_3|U(\boldsymbol{\theta})|\varphi_3\rangle|^2$. In this case, too, the algorithm succeeds in finding the third excited state of the Hamiltonian. However, the number of iterations to the convergence is larger than the number of overall iterations of the simple SSVQE. It might be attributed to the more complicated landscape existing in the cost function.

3. Weighted SSVQE

The weighted SSVQE described in Sec. II C can find $0, 1, \ldots, k$th excited states all at once. Here, we chose $\boldsymbol{w} =$
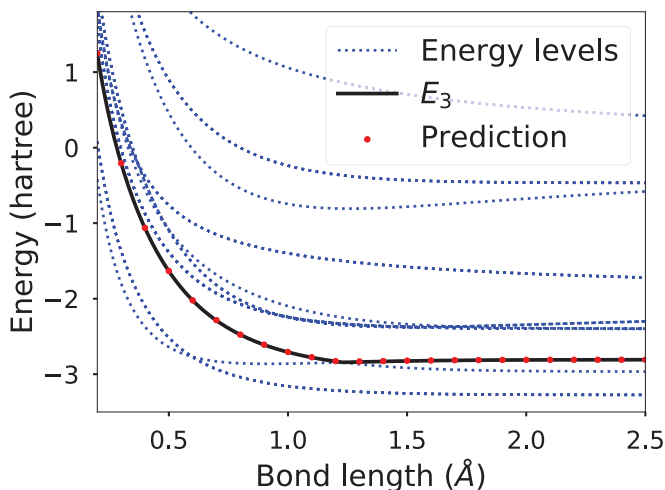

FIG. 7. The energy levels of the Hamiltonian of HeH and the predicted energy of the third excited state using the weighted SSVQE.
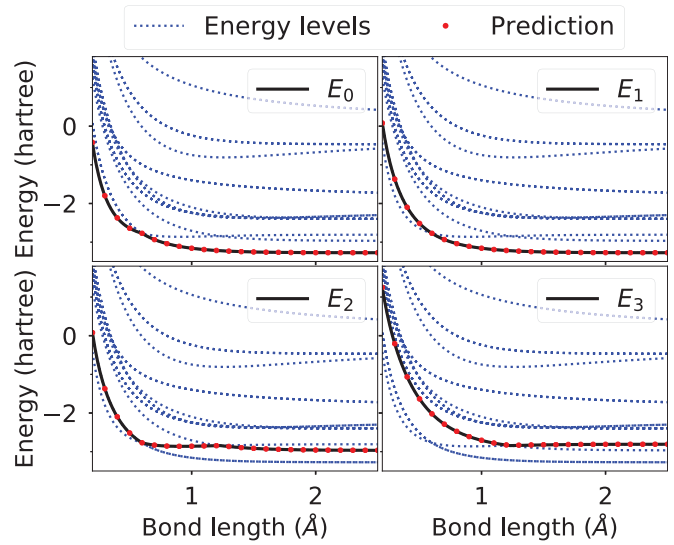

FIG. 8. The energy levels of the Hamiltonian of HeH and the predicted energy of the excited states up to the third using the weighted SSVQE. Upper left: Ground state; upper right: first excited state; lower left: second excited state; lower right: third excited state.

$(4, 3, 2, 1)$ as the weight vector. Figure 5 shows the optimization process of $\boldsymbol{\theta}$ to minimize $\mathcal{L}_{\boldsymbol{w}}(\boldsymbol{\theta})$. From Fig. 5, one can see that this approach can actually find the desired excited states all at once. The number of iterations to the convergence is almost equivalent to the one presented in the previous section.

B. Helium hydride

Next, we apply our idea for the molecular Hamiltonians of HeH with a fixed distance between two atoms. Our ansatz (Fig. 1) does not consider the conservation of the number of electrons, and therefore, the calculated excited states can have a different number of them. The molecular Hamiltonians are calculated with OPENFERMION and OPENFERMION-PSI4 [20,21]. We used the STO-3G minimal basis set, and therefore, obtained the 4-qubit Hamiltonian. We calculated the Hamiltonians at 24 different bond lengths and performed the VQE at each point. In the weighted SSVQE simulation, we used the same weights as in the previous section.

The result of SSVQE is shown in Fig. 6 and the one from using weighted SSVQE for finding the kth excited state is shown in Fig. 7. Both of the results agree nicely with the exact values of the third excited state at each bond length.

Next, we used the weighted SSVQE described in Sec. II C to find all excited states up to the third. The result is shown in Fig. 8. One can see that the energy eigenvalues are well approximated by the optimized output of the weighted SSVQE.

VI. CONCLUSION

In this work, we proposed efficient algorithms for finding the excited states of a given Hamiltonian, extending the framework of the VQE. The proposed method assures the orthogonality of the states at the input of the ansatz circuit. Minimizing a carefully designed cost function by optimizing the parameters of the quantum circuit, we can map each of

the orthogonal states onto one of the energy eigenstates. Our algorithms require us to run, in principle, optimization only once or twice, and find one or more arbitrary excited states. The depth of the ansatz required to perform accurate SSVQE might be greater than that of the conventional VQE. However, even for the conventional VQE, it is still not clear how the method depends on the circuit depth. One future direction can be to thoroughly analyze such dependency of the VQE and the proposed SSVQE by either numerical simulations or experiments. We believe that this work greatly extends the practicability of the VQE for finding the excited states.

APPENDIX: PROOF

Lemma A1. Let $\boldsymbol{x} = \begin{pmatrix} x_1 \\ x_2 \\ \vdots \\ x_n \end{pmatrix}$ and $\boldsymbol{y} = \begin{pmatrix} y_1 \\ y_2 \\ \vdots \\ y_n \end{pmatrix}$ be n-dimensional

vectors, and $A = \begin{pmatrix} a_{11} & \cdots & a_{1n} \\ \vdots & \ddots & \vdots \\ a_{n1} & \cdots & a_{nn} \end{pmatrix}$ be an $n \times n$ matrix.

If

$$x_1 \leqslant x_2 \leqslant \cdots \leqslant x_n, \tag{A1}$$

$$y_1 \leqslant y_2 \leqslant \cdots \leqslant y_n, \tag{A2}$$

$$a_{ij} \geqslant 0 \quad \text{for all } i, j \in \{1, \ldots, n\}, \tag{A3}$$

$$\sum_i a_{ij} = 1 \quad \text{for all } j \in \{1, \ldots, n\}, \tag{A4}$$

$$\sum_j a_{ij} = 1 \quad \text{for all } i \in \{1, \ldots, n\}, \tag{A5}$$

then

$$\boldsymbol{x}^T A \boldsymbol{y} \leqslant \boldsymbol{x}^T \boldsymbol{y}, \tag{A6}$$

and Eq. (A6) holds if and only if A satisfies the following equation,

$$A = \sum_j c'_j R_j^T Q_j, \tag{A7}$$

where the permutation matrix Q_j and R_j satisfies the following equations,

$$\boldsymbol{y} = Q_j \boldsymbol{y}, \quad \boldsymbol{x} = R_j \boldsymbol{x}. \tag{A8}$$

Proof. By the Birkhof–von Neumann theorem, A can be expanded as

$$A = \sum_i c_i P_i, \tag{A9}$$

where $\{P_i\}_i$ is the set of the $n \times n$ permutation matrices, $\sum_i c_i = 1, c_i \geqslant 0$ for all i.

By the rearrangement inequality,

$$\forall i \quad \boldsymbol{x}^T P_i \boldsymbol{y} \leqslant \boldsymbol{x}^T \boldsymbol{y} \quad [\because \text{(A1) and (A2)}]. \tag{A10}$$

Therefore,

$$\boldsymbol{x}^T A \boldsymbol{y} \leqslant \boldsymbol{x}^T \boldsymbol{y}. \tag{A11}$$

and Eq. (A6) holds if and only if A satisfies the following equation,

$$A = \sum_j c'_j R_j^T Q_j, \tag{A12}$$

where $\sum_j c'_j = 1, c'_j \geqslant 0$ for all j, and the permutation matrices Q_j and R_j satisfy the following equations,

$$\boldsymbol{y} = Q_j \boldsymbol{y}, \quad \boldsymbol{x} = R_j \boldsymbol{x}. \tag{A13}$$

∎

Theorem A2. We assume that $\{|\psi_i\rangle\}_{i=0}^{N-1}$ are orthonormal. Let $|e_i\rangle$ be the ith excited state of a given $N \times N$ Hamiltonian $\mathcal{H}$, and e_i is the energy of the ith excited state. When

$$\omega_0 \geqslant \omega_1 \geqslant \cdots \geqslant \omega_{N-1}, \tag{A14}$$

then

$$\sum_i \omega_i \langle \psi_i | \mathcal{H} | \psi_i \rangle \geqslant \sum_i \omega_i e_i, \tag{A15}$$

and Eq. (A15) holds if and only if the matrix B, the i, j elements of which is $|u_{ij}|$, satisfies the following equation,

$$B = \sum_j c'_k R_k^T Q_k, \tag{A16}$$

where $\sum_k c'_k = 1, c'_k \geqslant 0$ for all k, and the permutation matrix Q_k and R_k satisfies the following equations,

$$\boldsymbol{e} = Q_k \boldsymbol{e}, \quad \boldsymbol{\omega} = R_k \boldsymbol{\omega} \quad \left[\boldsymbol{e} := \begin{pmatrix} e_1 \\ e_2 \\ \vdots \\ e_n \end{pmatrix}, \boldsymbol{\omega} := \begin{pmatrix} \omega_1 \\ \omega_2 \\ \vdots \\ \omega_n \end{pmatrix} \right]. \tag{A17}$$

Proof. We rewrite ψ_i as follows:

$$|\psi_i\rangle = \sum_j a_{ij} |e_j\rangle. \tag{A18}$$

Then,

$$\sum_i u_{ij} = 1 \quad \text{for all } j, \tag{A19}$$

$$\sum_j u_{ij} = 1 \quad \text{for all } i, \tag{A20}$$

$$\sum_i \omega_i \langle \psi_i | \mathcal{H} | \psi_i \rangle = \sum_i \sum_j \omega_i e_j |u_{ij}|^2$$
$$= -\sum_i \sum_j (-\omega_i e_j)|u_{ij}|^2. \tag{A21}$$

By using Eqs. (A14) and (A19)–(A21), Lemma A1, and $e_0 \leqslant e_i \leqslant \cdots \leqslant e_{N-1}$, the above theorem can be shown. ∎

Note that the case in the main text where we only use k states instead of N states corresponds to the special case of the above theorem where $w_i = 0$ for all $i \geqslant k$.

[1] J. Preskill, Quantum **2**, 79 (2018).

[2] S. Boixo, S. V. Isakov, V. N. Smelyanskiy, R. Babbush, N. Ding, Z. Jiang, M. J. Bremner, J. M. Martinis, and H. Neven, Nat. Phys. **14**, 595 (2018).

[3] A. Bouland, B. Fefferman, C. Nirkhe, and U. Vazirani, arXiv:1803.04402.

[4] J. Chen, F. Zhang, C. Huang, M. Newman, and Y. Shi, arXiv:1805.01450.

[5] A. Peruzzo, J. McClean, P. Shadbolt, M.-H. Yung, X.-Q. Zhou, P. J. Love, A. Aspuru-Guzik, and J. L. O'Brien, Nat. Commun. **5**, 4213 (2014).

[6] B. Bauer, D. Wecker, A. J. Millis, M. B. Hastings, and M. Troyer, Phys. Rev. X **6**, 031045 (2016).

[7] A. Kandala, A. Mezzacapo, K. Temme, M. Takita, M. Brink, J. M. Chow, and J. M. Gambetta, Nature (London) **549**, 242 (2017).

[8] M. Klessinger and J. Michl, *Excited States and Photochemistry of Organic Molecules* (VCH, New York, 1995).

[9] H. Lischka, D. Nachtigallová, A. J. A. Aquino, P. G. Szalay, F. Plasser, F. B. C. Machado, and M. Barbatti, Chem. Rev. **118**, 7293 (2018).

[10] L. Serrano-Andrés and M. Merchán, J. Mol. Struct., Theochem **729**, 99 (2005).

[11] A. Dreuw and M. Head-Gordon, Chem. Rev. **105**, 4009 (2005).

[12] M. Reiher, N. Wiebe, K. M. Svore, D. Wecker, and M. Troyer, Proc. Natl. Acad. Sci. USA **114**, 7555 (2017).

[13] O. Higgott, D. Wang, and S. Brierley, Quantum **3**, 156 (2019).

[14] T. Jones, S. Endo, S. McArdle, X. Yuan, and S. Benjamin, Phys. Rev. A **99**, 062304 (2019).

[15] R. Santagati, J. Wang, A. A. Gentile, S. Paesani, N. Wiebe, J. R. McClean, S. Morley-Short, P. J. Shadbolt, D. Bonneau, J. W. Silverstone, D. P. Tew, X. Zhou, J. L. O'Brien, and M. G. Thompson, Sci. Adv. **4**, eaap9646 (2018).

[16] J. I. Colless, V. V. Ramasesh, D. Dahlen, M. S. Blok, M. E. Kimchi-Schwartz, J. R. McClean, J. Carter, W. A. de Jong, and I. Siddiqi, Phys. Rev. X **8**, 011021 (2018).

[17] I. G. Ryabinkin, S. N. Genin, and A. F. Izmaylov, arXiv:1806.00461.

[18] J. Nocedal and S. Wright, *Numerical Optimization*, Springer Series in Operations Research and Financial Engineering (Springer, New York, 2006).

[19] E. Jones, T. Oliphant, P. Peterson *et al.*, SciPy: Open source scientific tools for Python (2001), http://www.scipy.org/

[20] J. R. McClean, I. D. Kivlichan, K. J. Sung, D. S. Steiger, Y. Cao, C. Dai, E. S. Fried, C. Gidney, B. Gimby, P. Gokhale, T. Häner, T. Hardikar, V. Havlíček, C. Huang, J. Izaac, Z. Jiang, X. Liu, M. Neeley, T. O'Brien, I. Ozfidan *et al.*, arXiv:1710.07629.

[21] R. M. Parrish, L. A. Burns, D. G. A. Smith, A. C. Simmonett, A. E. DePrince, E. G. Hohenstein, U. Bozkaya, A. Y. Sokolov, R. Di Remigio, R. M. Richard, J. F. Gonthier, A. M. James, H. R. McAlexander, A. Kumar, M. Saitow, X. Wang, B. P. Pritchard, P. Verma, H. F. Schaefer, K. Patkowski *et al.*, J. Chem. Theory Comput. **13**, 3185 (2017).

[22] https://qunasys.com/